Mesoporous alumina molecular sieves: characterization and catalytic activity in hydrolysis of carbon disulfide

Xiping Zhao, Yinghong Yue, Ying Zhang, Weiming Hua, and Zi Gao*

Laboratory of Molecular Catalysis and Innovative Materials, Department of Chemistry, Fudan University, Shanghai 200433, P.R. China

Received 16 January 2003; accepted 21 April 2003

Mesoporous MSU-X alumina molecular sieves were synthesized through the neutral N^0I^0 assembly pathway using aluminum *sec*-butoxide as the precursor and a triblock poly(ethylene glycol)-poly(propylene glycol)-poly(ethylene glycol) as the structure-directing agent. Their surface acidity and basicity as well as textural properties were characterized by NH_3-TPD, CO_2-TPD, IR spectroscopy and N_2 adsorption methods. The materials are abundant in surface weak acid sites and weak-medium basic sites. They are more active than the commercial γ-Al_2O_3 catalyst for the CS_2 hydrolysis reaction, and the temperature of 90% conversion of CS_2 on the mesoporous alumina is 130 K lower than that of γ-Al_2O_3.

KEY WORDS: mesoporous MSU-X alumina molecular sieve; surface acidity and basicity; CS_2 hydrolysis.

1. Introduction

The synthesis of mesoporous silica with high surface area and uniform cylindrical mesopores, which was designated as M41S, was first demonstrated in 1992 [1]. Since then, the use of surfactants and amphiphilic block copolymers to organize mesoporous structures has been extended to the preparation of non-silica mesoporous metal oxides. Mesoporous MnO_2 [2], Al_2O_3 [3–6], TiO_2 [6,7], Nb_2O_5 [6,8], Ta_2O_5 [6,8], ZrO_2 [6,9] and SnO_2 [6,10] have been synthesized successfully over the past few years. Among them, mesoporous Al_2O_3 is of particular interest because high surface area aluminas are important industrial catalysts and catalyst supports.

Mesoporous alumina molecular sieves can be prepared by electrostatic assembly pathways, i.e., using electrostatic interactions between a positively charged surfactant and a negatively charged inorganic precursor (S^+I^-) or charge-reversed interactions (S^-I^+) to assemble the mesostructure. For example, Yada *et al.* [4] reported the preparation of hexagonal alumina mesostructures by electrostatic (S^-I^+) assembly of dodecyl sulfate anionic surfactant and aluminum nitrate, and Cabrara *et al.* [5] prepared mesostructure alumina using cationic cetyltrimethylammonium bromide as a surfactant-directing agent in a water/triethanolamine medium. Mesoporous alumina molecular sieves can also be obtained via neutral assembly pathways (N^0I^0) using nonionic templates [3]. Neutral pathways have many advantages over electrostatic pathways; especially, templates which are easier to remove due to the weak interactions between the template and the framework wall. Recently, a rare earth stabilized mesoporous alumina molecular sieve designated as MSU-X has been synthesized using a triblock poly(ethylene glycol)-poly(propylene glycol)-poly(ethylene glycol) as a structure-directing agent through the N^0I^0 assembly pathway [11]. The high surface area, large pore volume and high stability of the mesostructure are attractive in designing catalysts for numerous reactions.

The Clause process is widely used to convert H_2S effluent to elemental sulfur. A considerable amount of carbon disulfide is formed in this process because of the coexistence of hydrocarbon impurities in the effluent, leading to harmful emissions into the atmosphere [12,13]. Catalytic hydrolysis is an effective way to remove CS_2 [14], and alumina is an industrial catalyst for this reaction [14–17]. In this work, mesoporous MSU-X alumina molecular sieves were prepared by the N^0I^0 method at different template/aluminum precursor ratios. Their acidity, basicity and textural properties were characterized by NH_3-TPD, CO_2-TPD, IR spectroscopy and N_2 adsorption methods. The catalytic activities of the mesoporous alumina molecular sieves towards carbon disulfide hydrolysis were tested at ambient pressure and compared with that of the commercial γ-Al_2O_3 catalyst.

2. Experimental

2.1. Sample preparation

The mesoporous MSU-X alumina molecular sieves were prepared following the procedure in the literature [11]: A calculated amount of triblock poly(ethylene glycol)-poly(propylene glycol)-poly(ethylene glycol) ($EO_{20}PO_{70}EO_{20}$, Aldrich) together with 0.060 g$LaCl_3$

* To whom correspondence should be addressed.
E-mail: zigao@fudan.edu.cn

1011-372X/03/0700–0041/0

was dissolved in 25 mL *sec*-butanol, and then 5.4 mL aluminum *sec*-butoxide was added with stirring. After stirring for 1 h at ambient temperature, a dilute solution of water in *sec*-butanol (1.14 mL H_2O/10 mL *sec*-butanol) was added dropwise. The molar composition of the final reaction mixture was $0.01\,La^{3+}$: $1.0\,Al(Bu^sO)_3$: $(0.05 \sim 0.20)EO_{20}PO_{70}EO_{20}$: $3.0\,H_2O$: $15.5\,Bu^sOH$. The mixture was stirred at 318 K for another 48 h. The product obtained was filtered, dried in air and calcined at 773 K for 6 h in flowing air. The mesoporous MSU-X alumina prepared via N^0I^0 assembly is designated as *meso*-Al_2O_3-*a*.

For comparison, another type of mesoporous alumina was prepared as follows using CTABr (cetyltrimethyl ammonium bromide) as a surfactant-directing agent [5]: (1) A solution containing 0.4 g of NaOH in 2 mL H_2O was added to 40 mL triethanolamine and heated at 393 K for 5 min to evaporate the water. Over this solution, 10.9 mL aluminum *sec*-butoxide was added dropwise with stirring. The resulting solution was then heated at 423 K for 10 min (solution I). (2) 7.28 g CTABr was dissolved in 120 mL H_2O at 333 K (solution II). (3) Solution I was slowly added to solution II with vigorous stirring at 333 K, and the mixture was allowed to age for another 72 h. The precipitate was filtered, washed with ethanol, dried at 303 K and calcined at 773 K for 5 h in flowing air. The mesoporous alumina prepared via S^+I^- assembly is designated as *meso*-Al_2O_3-*b*.

2.2. Characterization

X-ray powder diffraction (XRD) patterns of the samples were obtained on a Rigaku D/MAX-IIA diffractometer using CuKα radiation at 30 kV and 20 mA. The N_2 adsorption/desorption isotherms were measured on a Micromeritics ASAP-2000 instrument at liquid N_2 temperature. Specific surface areas of the samples were calculated from the adsorption isotherms by the BET method, and pore size distributions from the desorption isotherms by the BJH method. Transmission electron microscopy (TEM) was conducted on a JEOL-2011 instrument. The temperature-programmed desorption of NH_3 (NH_3-TPD) of the samples was carried out in a flow-type fixed-bed reactor. The NH_3 adsorption temperature was 393 K, and the temperature was raised at a rate of 10 K/min. The desorbed NH_3 was collected in a liquid N_2 trap and detected by gas chromatography. The temperature-programmed desorption of CO_2 (CO_2-TPD) was measured on the same instrument. The CO_2 adsorption temperature was 353 K, and the temperature was raised to 773 K at a rate of 10 K/min. The desorbed CO_2 was also collected in a liquid N_2 trap and detected by gas chromatography. For infrared spectroscopic (IR) study, self-supporting wafers with a density of ca. 3.2 mg/cm^2 of the catalysts were prepared. IR spectrum was recorded on a Perkin-Elmer 983G spectrometer after evacuation at 523 K.

2.3. Activity tests

The dehydration of isopropanol was performed in a pulsed microreactor with a catalyst load of 50 mg. The catalyst was preheated in H_2 flow at 773 K for 2.5 h. H_2 was used as the carrier gas at a flow rate of 60 mL/min. The amount of isopropanol injected for each test was 5 μL and the reaction temperatures were 523, 573, 623 and 648 K. The products were analyzed by an on-line gas chromatograph equipped with a thermal conductivity detector (TCD) and a 2-m column of GDX-301.

The CS_2 hydrolysis reaction was conducted in a continuous fixed-bed flow micro-reactor at ambient pressure. 0.8 g of the catalysts granulated into $40 \sim 60$ mesh was pretreated in flowing N_2 at 723 K for 1.5 h before reaction. 1 mol% CS_2, 10 mol% H_2O and balance N_2 were mixed and passed through the reactor at a space velocity (GHSV) of 1000 h^{-1}. The products were analyzed by an on-line gas chromatograph equipped with a flame ionization detector (FID) and a 2-m column of PEG 6000, and the main hydrolysis products were H_2S and CO_2. No SO_2 and COS were detected for all the catalysts.

3. Results and discussion

3.1. Structural characterization

Mesoporous MSU-X alumina molecular sieves were prepared at triblock copolymer/Al precursor molar ratios of 0.05, 0.10 and 0.20. Their textural properties were characterized by the N_2 adsorption/desorption method. The isotherms and pore size distribution curves of three *meso*-Al_2O_3-*a* samples look very similar, so only the isotherms and pore size distribution curves of *meso*-Al_2O_3-*a*2, *meso*-Al_2O_3-*b* and the commercial γ-Al_2O_3 are illustrated in figures 1 and 2. The isotherm of *meso*-Al_2O_3-*a*2 is of type IV with a typical H1 hysteresis loop appearing in the P/P_0 range of 0.6–0.9, and the sample has a narrow pore size distribution centered at 5.8 nm. The isotherm of *meso*-Al_2O_3-*b* prepared with CTABr as the surfactant-directing agent is somewhat different from that of *meso*-Al_2O_3-*a*2. Its hysteresis loop is much smaller and appears in the P/P_0 range of 0.4–0.8, indicating a reduction in pore diameter and pore volume. Moreover, the sharp curvature of the desorption isotherm of *meso*-Al_2O_3-*b* suggests the existence of some necking in the pore structure. The isotherm of the γ-Al_2O_3 sample is of type V with a H3 hysteresis loop characteristic of an aggregate of nano-sized nonporous particles, and the pore size distribution of the sample is rather broad.

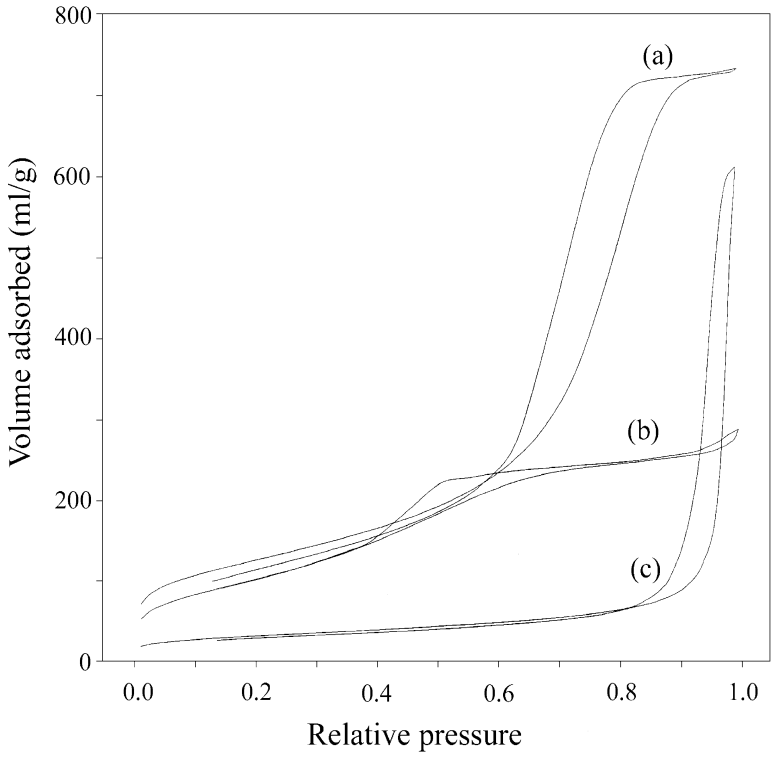

Figure 1. N_2 adsorption and desorption isotherms of (a) *meso*-Al_2O_3-*a*2, (b) *meso*-Al_2O_3-*b* and (c) γ-Al_2O_3.

The specific surface area, pore volume and the most probable pore diameter of all the samples are summarized in table 1 for comparison. Obviously, the rare earth stabilized mesoporous MSU-X alumina molecular sieves obtained via the N^0I^0 assembly pathway have a higher specific surface area, larger pore volume and wider pore diameter than those of the others, and $EO_{20}PO_{70}EO_{20}$/Al molar ratio of 0.10 is a good choice for the preparation of such materials.

The TEM images of calcined *meso*-Al_2O_3-*a*2 and *meso*-Al_2O_3-*b* are given in figure 3. The regular worm-like channels with no discernible long-range packing

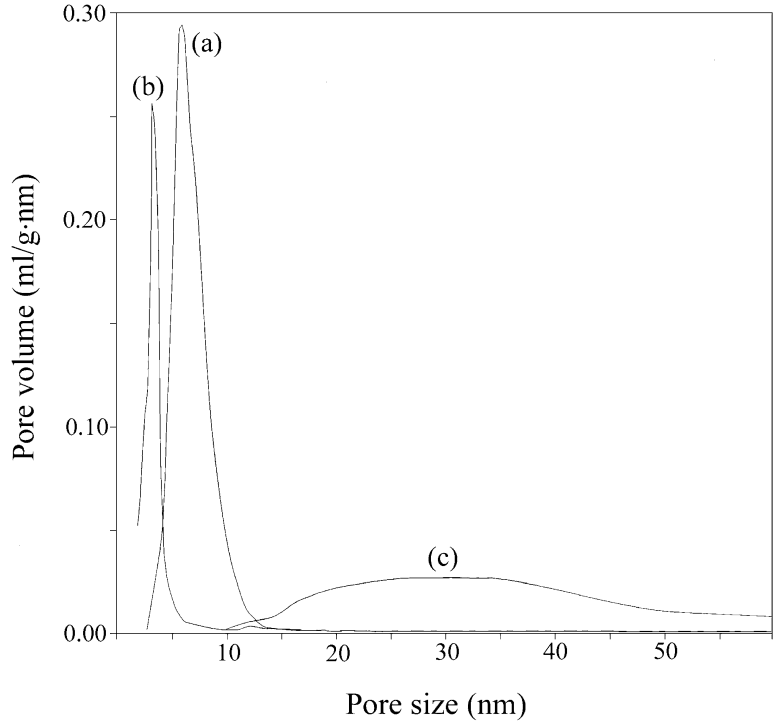

Figure 2. Pore size distributions of (a) *meso*-Al_2O_3-*a*2, (b) *meso*-Al_2O_3-*b* and (c) γ-Al_2O_3.

Table 1
Textural properties of the alumina samples

Samples	$EO_{20}PO_{70}EO_{20}$/Al (mol/mol)	Surface area (m^2/g)	Pore volume (mL/g)	Pore diameter (nm)
meso-Al_2O_3-*a*1	0.20	485	1.05	4.7
meso-Al_2O_3-*a*2	0.10	446	1.12	5.8
meso-Al_2O_3-*a*3	0.05	443	0.82	5.7
meso-Al_2O_3-*b*	–	368	0.40	4.1
γ-Al_2O_3	–	108	0.43	29

Table 2
Results of NH_3-TPD and the isopropanol dehydration reaction

Samples	NH_3-TPD		Isopropanol conversion (%)			
	Peak temperature (K)	NH_3 desorbed (mmol/g)	523 K	573 K	623 K	648 K
meso-Al_2O_3-*a*2	546	0.645	6.7	28.5	68.9	85.9
meso-Al_2O_3-*b*	563	0.640	8.2	30.0	72.3	86.7
γ-Al_2O_3	623	0.395	37.1	80.5	100	100

order are observed for *meso*-Al_2O_3-*a*2. This is very similar to that of *meso*-Al_2O_3-*b*, in which no apparent order but "sponge-like" in pore arrangement exists. Selected-area electron diffraction patterns recorded on these two samples (figure 3, inset) show that both channel walls are amorphous in nature. Wide-angle X-ray diffraction patterns of the two calcined samples also indicate that the channel walls are amorphous. These results are consistent with those reported by Pinnavaia [11] and Cabrara [5].

3.2. Acidity measurement

The surface acidity of *meso*-Al_2O_3-*a*2, *meso*-Al_2O_3-*b* and γ-Al_2O_3 was measured by the NH_3-TPD method. There is only one asymmetric broad peak on the NH_3-TPD profiles of the samples. The peak temperature and the amount of NH_3 desorbed for the samples are given in table 2. The number of surface acid sites on the two mesoporous alumina samples is much greater than that on γ-Al_2O_3, but the desorption peak temperature of the former is much lower than that on the latter, indicating that the mesoporous alumina samples are more abundant in weak surface acid sites owing to their high surface area and amorphous channel walls.

The dehydration of isopropanol was used as a catalytic probe reaction to test the acidity of the samples as well. Propylene is the only reaction product obtained on all the catalysts. The isopropanol conversions at different reaction temperatures for the catalysts are

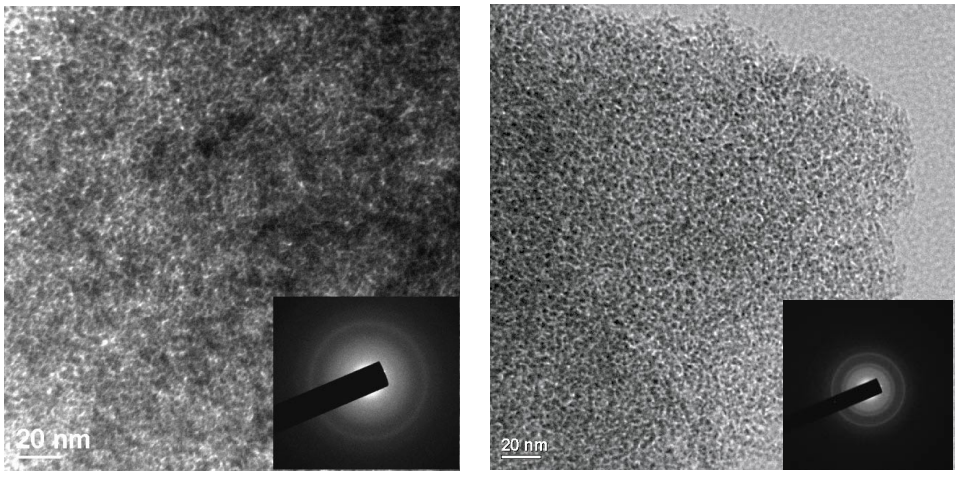

(a) (b)

Figure 3. TEM images and selected-area electron diffraction patterns (inset) of (a) *meso*-Al_2O_3-*a*2 and (b) *meso*-Al_2O_3-*b*.

Table 3
Results of CO_2-TPD and the CS_2 hydrolysis reaction

Samples	CO_2-TPD		CS_2 hydrolysis	
	Peak temperature (K)	CO_2 desorbed (mmol/g)	T_{50} (K)	T_{90} (K)
meso-Al_2O_3-*a*2	428	0.0636	398	483
meso-Al_2O_3-*b*	430	0.0595	423	513
γ-Al_2O_3	438	0.0133	483	613

listed in table 2. γ-Al_2O_3 is more active than the two mesoporous alumina catalysts for isopropanol dehydration especially at lower temperatures because of the stronger acid strength of the surface acid sites.

3.3. Basicity measurement

The surface basicity of *meso*-Al_2O_3-*a*2, *meso*-Al_2O_3-*b* and γ-Al_2O_3 was measured by the CO_2-TPD method. There is also only one asymmetric broad peak on the CO_2-TPD profiles of the samples. The peak temperature and the amount of CO_2 desorbed for the samples are listed in table 3. The number of surface basic sites on the two mesoporous alumina samples is much greater than that on γ-Al_2O_3, but the CO_2 desorption peak temperatures of all the alumina samples are close to each other. This shows that the mesoporous alumina samples are more abundant in surface basic sites owing to their high surface area. However, unlike the acid sites, the strength of the base sites of the mesoporous aluminas is little affected by the amorphous state of the channel walls, and it is close to that of γ-Al_2O_3.

The infrared adsorptions of the hydroxyl groups on *meso*-Al_2O_3-*a*2 and γ-Al_2O_3 were measured after evacuation at 523 K. The spectra of the two samples are similar (figure 4), presenting an intense broad band centered around 3580 cm^{-1} accompanied by two shoulder peaks at 3679 and 3730 cm^{-1}. The OH bands at 3730 and 3679 cm^{-1} are assigned to free hydroxyl groups, whereas the 3580 cm^{-1} band is assigned to hydrogen-bonded hydroxyl groups [16]. The relative intensities of the free hydroxyl group vibrations of *meso*-Al_2O_3-*a*2 are evidently higher than those of γ-Al_2O_3. The free hydroxyl groups are usually the active basic sites in catalytic reactions, and the abundance of basic hydroxyl groups on *meso*-Al_2O_3-*a*2 samples is favorable for them to act as good catalysts for base-catalyzed reactions.

3.4. CS_2 hydrolysis

CS_2 hydrolysis is an important chemical process in environmental technology, and γ-Al_2O_3 is the industrial catalyst for the process. The catalytic activities of mesoporous alumina molecular sieves for CS_2 hydrolysis are compared with that of γ-Al_2O_3 under the same reaction conditions. The conversion of CS_2 on the catalysts increases with reaction temperature as shown in figure 5. The temperatures at which 50% (T_{50}) and 90% (T_{90}) of CS_2 are converted are taken as a measure of the hydrolysis activity of the catalysts and are given in table 3. The hydrolysis activity of the catalysts follows the order of *meso*-Al_2O_3-*a*2 > *meso*-Al_2O_3-*b* > γ-Al_2O_3. The T_{90} of *meso*-Al_2O_3-*a*2 is 130 K lower than that of γ-Al_2O_3.

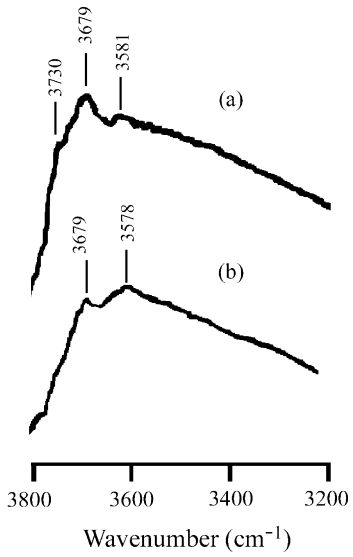

Figure 4. IR spectra of (a) *meso*-Al_2O_3-*a*2 and (b) γ-Al_2O_3.

Mechanistic studies of the hydrolysis reaction of CS_2 suggest that the sulfide adsorbs onto the basic hydroxyl groups on the surface of the catalysts and a hydrogen thiocarbonate intermediate is formed [14,16,17]. The intermediate reacts with water to form H_2S and CO_2. Therefore, the hydrolysis activity is related to the concentration of the surface basic hydroxyl sites on the catalysts. The abundance of surface basic hydroxyl groups on *meso*-Al_2O_3-*a*2 explains its high catalytic activity for the reaction.

The catalytic stability of *meso*-Al_2O_3-*a*2 and γ-Al_2O_3 for CS_2 hydrolysis was tested as well. The reaction was carried out at their T_{90} temperature, i.e., 483 K and 613 K respectively. The results are shown in figure 6. Both catalysts are stable within the test period.

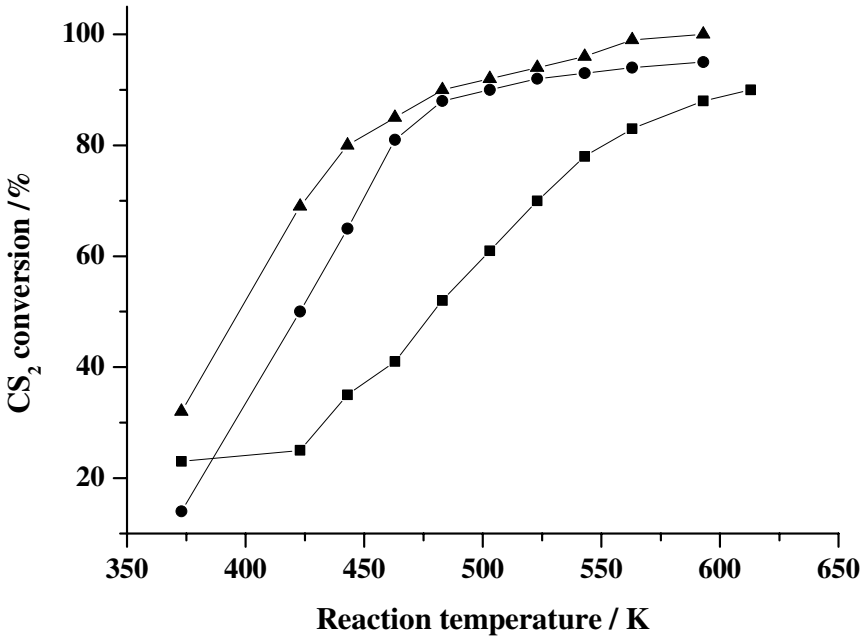

Figure 5. CS_2 hydrolysis activities of (▲) *meso*-Al_2O_3-*a*2, (●) *meso*-Al_2O_3-*b* and (■) γ-Al_2O_3 as a function of reaction temperature.

4. Conclusions

Mesoporous MSU-X alumina molecular sieves prepared via the N^0I^0 assembly pathway have high thermal stability, large surface area and uniform mesoporosity. More importantly, they are abundant in surface weak acid sites and weak-medium basic sites, offering promising opportunities as catalysts for acid- and base-catalyzed reactions. The present work shows that *meso*-Al_2O_3-*a*2 prepared by the N^0I^0 assembly pathway is more active than *meso*-Al_2O_3-*b* prepared by the S^+I^- assembly pathway for CS_2 hydrolysis, and both mesoporous aluminas are much more active than the commercial γ-Al_2O_3 catalyst for the reaction. The temperature of 90% conversion of CS_2 on *meso*-Al_2O_3-*a*2 is 130 K lower than that of γ-Al_2O_3, and the catalyst is rather stable on stream.

Acknowledgment

This work was supported by the Chinese Major State Basic Research Development Program (Grant no. 2000077507) and the Foundation for University Key Teachers by the Chinese Ministry of Education.

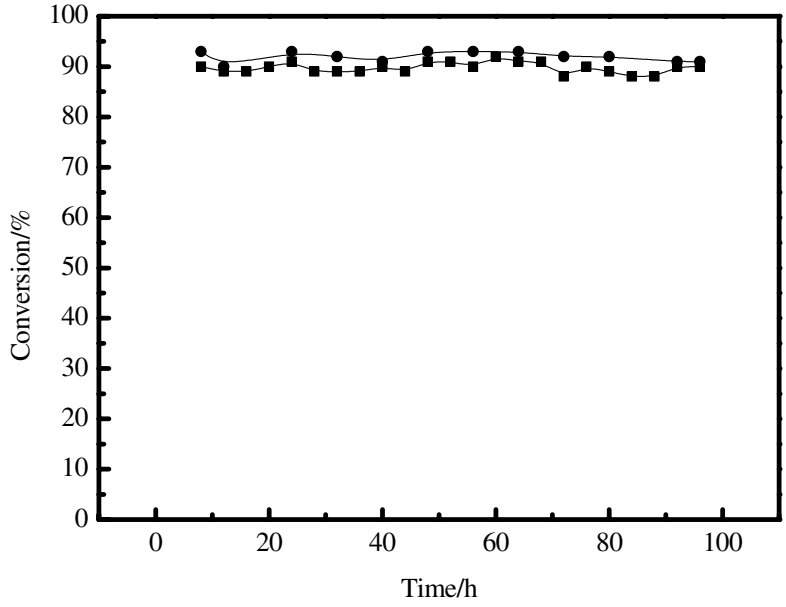

Figure 6. Catalytic stability test on (■) *meso*-Al_2O_3-*a*2 at 483 K and (●) γ-Al_2O_3 at 613 K.

References

[1] C.T. Kresge, M.E. Leonowicz, W.J. Roth, J.C. Vartuli and J.S. Beck, Nature 359 (1992) 710.
[2] Z. Tian, W. Tong, J. Wang, N. Duan, V.V. Krishnan and S.L. Suib, Science 276 (1997) 926.
[3] S.A. Bagshaw and T.J. Pinnavaia, Angew. Chem., Int. Ed. Engl. 35 (1996) 1102.
[4] M. Yada, M. Machida and T. Kijima, Chem. Commun. (1996) 1451.
[5] S. Cabrara, J.E. Haskouri, J. Alamo, A. Beltran, D. Beltran, S. Mendioroz, M.D. Marcos and P. Amoros, Adv. Mater. 11 (1999) 379.
[6] P. Yang, D. Zhao, D.I. Margolese, B.F. Chmelka and D.G. Stucky, Chem. Mater. 11 (1999) 2813.
[7] D.M. Antonelli and J.Y. Ying, Angew. Chem., Int. Ed. Engl. 34 (1995) 2014.
[8] D.M. Antonelli and J.Y. Ying, Chem. Mater. 8 (1996) 874.
[9] J.A. Knowles and M.J. Hudson, Chem. Commun. (1995) 2083.
[10] K.G. Severin, T.M. AbdelFattah and T.J. Pinnavaia, Chem. Commun. (1998) 1471
[11] W. Zhang and J. Pinnavaia, Chem. Commun. (1998) 1185.
[12] T.T. Chung, J.G. Dalla Lana and C.L. Lui, J. Chem. Soc., Faraday Trans. 1. 69 (1972) 643.
[13] M.J. Pearson, Hydrocarbon Process. 60 (1981) 131.
[14] C. Rhodes, S.A. Riddel, J. West, B.P. Williams and G.J. Hutchings, Catal. Today 59 (2000) 443.
[15] P.D. Clark, N.I. Dowling and M. Huang, Appl. Catal., B: Environ. 31 (2001) 107.
[16] P.E. Hoggan, A. Aboulayt, A. Pieplu, P. Nortier and J.C. Lavalley, J. Catal. 149 (1994) 300.
[17] R. Fiedorow, R. Leaute and I.G. Dalla Lana, J. Catal. 85 (1984) 339.